Computers and Mathematics with Applications 62 (2011) 3343–3352

Contents lists available at SciVerse ScienceDirect

Computers and Mathematics with Applications

journal homepage: www.elsevier.com/locate/camwa

Unsteady flow of a reactive variable viscosity non-Newtonian fluid through a porous saturated medium with asymmetric convective boundary conditions

O.D. Makinde [a], T. Chinyoka [b,*], L. Rundora [a]

[a] *Institute for Advance Research in Mathematical Modelling and Computations, Cape Peninsula University of Technology, P. O. Box 1906, Bellville 7535, South Africa*

[b] *Center for Research in Computational and Applied Mechanics, University of Cape Town, Rondebosch 7701, South Africa*

ARTICLE INFO

Article history:
Received 24 November 2010
Received in revised form 19 August 2011
Accepted 22 August 2011

Keywords:
Unsteady reactive flow
Saturated porous medium
Third-grade fluid
Variable viscosity
Convective boundary conditions
Finite difference method

ABSTRACT

This article examines the thermal effects in an unsteady flow of a pressure driven, reactive, variable viscosity, third-grade fluid through a porous saturated medium with asymmetrical convective boundary conditions. We assume that exothermic chemical reactions take place within the flow system and that the asymmetric convective heat exchange with the ambient at the surfaces follow Newton's law of cooling. The coupled nonlinear partial differential equations governing the problem are derived and solved numerically using a semi-implicit finite difference scheme. Graphical results are presented and discussed qualitatively and quantitatively with respect to various parameters embedded in the problem.

1. Introduction

Flow of reactive fluids in porous media not only presents a theoretically challenging problem but also finds a wide range of technological and engineering applications [1]. This type of flow system can, for example, be found in packed bed chemical reactors, geothermal reservoirs, petroleum reservoirs, material processing industries, automobile exhaust systems, etc. Moreover, there are manifestations of fluid behavior which cannot be adequately explained on the basis of the classical, linearly viscous model [2]. Geological materials, liquid foams, polymeric fluids, slurries, drilling mud, clay coatings, elastomers, many emulsions, hydrocarbon oils, grease, and food products are among the many substances which are capable of flowing but which exhibit flow characteristics that cannot be adequately described by the classical linearly viscous fluid model. In order to describe some of the departures from Newtonian behavior evidenced by such materials, a number of idealized material models have been suggested. Amongst these are fluids of the differential type of third grade [3,4]. Meanwhile, the evaluation of thermal effects of a reactive non-Newtonian fluid in a porous medium is extremely important in order to ensure safety of life and property during handling and processing of such fluids [5,6]. Al-Hadhrami et al. [7] studied the thermal effects of steady flow of a Newtonian fluid in porous media across a range of permeability values. The pioneering papers by Aziz [8], and Makinde and Aziz [9], and the references therein introduced the idea of using the convective boundary conditions in boundary layer flows. We adopt such boundary conditions in the current work. Makinde [10,11] investigated the thermal effects of a reactive viscous flow through a channel filled with porous medium and with isothermal walls. Several studies involving heat and mass transfer in non-Newtonian third-grade fluids have been

* Corresponding author.
E-mail addresses: makinded@cput.ac.za (O.D. Makinde), tchinyok@vt.edu (T. Chinyoka).

0898-1221/$ – see front matter © 2011 Elsevier Ltd. All rights reserved.
doi:10.1016/j.camwa.2011.08.049

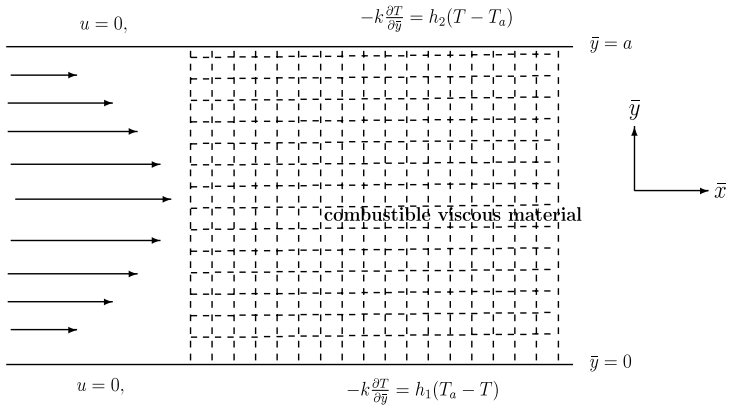

Fig. 1. Geometry of the problem.

conducted [12–14], but most of these studies seem to lack a systematic and rational treatment of the thermodynamics of the problem with respect to the combined effects of porous media, unsteadiness, variable viscosity and asymmetric convective boundary conditions on the flow system.

The objective of the present work is to study the unsteady flow of a reactive variable viscosity third-grade fluid between two parallel plates filled with a porous medium. Both the lower and upper walls of the channel are subjected to asymmetric convective heat exchange with the ambient. The mathematical formulation of the problem is established in Section 2. In Section 3 the semi-implicit finite difference technique is implemented in the process of solution of the problem. Graphical results are presented and discussed qualitatively and quantitatively with respect to various parameters embedded in the system in Section 4.

2. The mathematical model

Consider an unsteady flow of an incompressible, third-grade, variable viscosity, reactive fluid through a channel filled with a homogeneous and isotropic porous medium as illustrated in Fig. 1. It is assumed that the plate surfaces are subjected to asymmetric convective heat exchange with the ambient due to unequal heat transfer coefficients and the fluid motion is induced by an applied axial pressure gradient. We choose the $\bar{x}$-axis parallel to the channel and the $\bar{y}$-axis normal to it.

Following [1–7], and neglecting the reacting viscous fluid consumption, the governing equations for the momentum and heat balance can be written as

$$\rho\frac{\partial u}{\partial \bar{t}} = -\frac{\partial \bar{P}}{\partial \bar{x}} + \frac{\partial}{\partial \bar{y}}\left[\bar{\mu}(T)\frac{\partial u}{\partial \bar{y}}\right] + \alpha_1\frac{\partial^3 u}{\partial \bar{y}^2\partial \bar{t}} + 6\beta_3\frac{\partial^2 u}{\partial \bar{y}^2}\left(\frac{\partial u}{\partial \bar{y}}\right)^2 - \frac{\bar{\mu}(T)u}{\rho K} \tag{1}$$

$$\rho\, c_p\frac{\partial T}{\partial \bar{t}} = k\frac{\partial^2 T}{\partial \bar{y}^2} + \left(\frac{\partial u}{\partial \bar{y}}\right)^2\left(\bar{\mu}(T) + 2\beta_3\left(\frac{\partial u}{\partial \bar{y}}\right)^2\right) + \frac{\bar{\mu}(T)u^2}{K} + QC_0A\left(\frac{hT}{\nu l}\right)^m \mathrm{e}^{-\frac{E}{RT}}. \tag{2}$$

The additional viscous dissipation term in Eq. (2) is due to Al-Hadhrami et al. [7] and is valid in the limit of very small and very large porous medium permeability. The appropriate initial and boundary conditions are

$$u(\bar{y}, 0) = 0, \qquad T(\bar{y}, 0) = T_0, \tag{3}$$

$$u(0, \bar{t}) = 0, \qquad -k\frac{\partial T}{\partial \bar{y}}(0, \bar{t}) = h_1[T_a - T(0, \bar{t})], \tag{4}$$

$$u(a, \bar{t}) = 0, \qquad -k\frac{\partial T}{\partial \bar{y}}(a, \bar{t}) = h_2[T(a, \bar{t}) - T_a]. \tag{5}$$

Here T is the absolute temperature, ρ is the density, c_p is the specific heat at constant pressure, $\bar{t}$ is the time, h_1 is the heat transfer coefficient at the lower plate, h_2 is the heat transfer coefficient at the upper plate, T_0 is the fluid initial temperature, T_a is the ambient temperature, k is the thermal conductivity of the material, Q is the heat of reaction, A is the rate constant, E is the activation energy, R is the universal gas constant, C_0 is the initial concentration of the reactant species, a is the channel width, l is Planck's number, h is Boltzmann's constant, ν is the vibration frequency, K is the porous medium permeability, α_1 and β_3 are the material coefficients, $\bar{P}$ is the modified pressure, and m is the numerical exponent such that $m \in \{-2, 0, 0.5\}$, where the three values represent numerical exponents for sensitized, Arrhenius and bimolecular kinetics respectively (see [6,10,11]). The temperature dependent viscosity ($\bar{\mu}$) can be expressed as

$$\bar{\mu}(T) = \mu_0\mathrm{e}^{-b(T-T_0)}, \tag{6}$$

where b is a viscosity variation parameter and μ_0 is the initial fluid dynamic viscosity at temperature T_0. We introduce the following dimensionless variables into Eqs. (1)–(6);

$$y = \frac{\bar{y}}{a}, \quad \alpha = \frac{bRT_0^2}{E}, \quad W = \frac{u\rho a}{\mu_0}, \quad \theta = \frac{E(T-T_0)}{RT_0^2}, \quad \theta_a = \frac{E(T_a-T_0)}{RT_0^2},$$
$$\gamma = \frac{\beta_3\mu_0}{\rho^2 a^4}, \quad \delta = \frac{\alpha_1}{\rho a^2}, \quad \mathrm{Bi}_1 = \frac{h_1 a}{k}, \quad \mathrm{Bi}_2 = \frac{h_2 a}{k}, \quad \mathrm{Da} = \frac{K}{a^2}, \quad \mathrm{Pr} = \frac{\mu_0 c_p}{k},$$
$$\varepsilon = \frac{RT_0}{E}, \quad x = \frac{\bar{x}}{a}, \quad P = \frac{\bar{P}\rho a^2}{\mu_0^2}, \quad G = -\frac{\partial \bar{P}}{\partial x}, \quad S^2 = \frac{1}{\mathrm{Da}}, \quad t = \frac{\bar{t}\mu_0}{\rho a^2},$$
$$\mu = \frac{\bar{\mu}}{\mu_0}, \quad \lambda = \left(\frac{hT_0}{\nu l}\right)^m \frac{QEAa^2C_0 e^{-\frac{E}{RT}}}{T_0^2 Rk}, \quad \Omega = \left(\frac{\nu l}{hT_0}\right)^m \frac{\mu_0^3 e^{\frac{E}{RT}}}{\rho^2 QAa^4 C_0} \tag{7}$$

and obtain the following dimensionless governing equations:

$$\frac{\partial W}{\partial t} = G - S^2 W e^{-\alpha\theta} + e^{-\alpha\theta}\frac{\partial^2 W}{\partial y^2} - \alpha e^{-\alpha\theta}\frac{\partial\theta}{\partial y}\frac{\partial W}{\partial y} + \delta\frac{\partial^3 W}{\partial y^2 \partial t} + 6\gamma\frac{\partial^2 W}{\partial y^2}\left(\frac{\partial W}{\partial y}\right)^2, \tag{8}$$

$$\mathrm{Pr}\,\frac{\partial\theta}{\partial t} = \frac{\partial^2\theta}{\partial y^2} + \lambda\left\{(1+\varepsilon\theta)^m \exp\left(\frac{\theta}{1+\varepsilon\theta}\right) + \Omega\left[S^2 W^2 e^{-\alpha\theta} + \left(\frac{\partial W}{\partial y}\right)^2\left(e^{-\alpha\theta} + 2\gamma\left(\frac{\partial W}{\partial y}\right)^2\right)\right]\right\}, \tag{9}$$

$$W(y,0) = 0, \quad \theta(y,0) = 0, \tag{10}$$

$$W(0,t) = 0, \quad \frac{\partial\theta}{\partial y}(0,t) = -\mathrm{Bi}_1\,[\theta_a - \theta(0,t)], \tag{11}$$

$$W(1,t) = 0, \quad \frac{\partial\theta}{\partial y}(1,t) = -\mathrm{Bi}_2\,[\theta(1,t) - \theta_a], \tag{12}$$

where λ, Pr, Bi, ε, δ, γ, G, Da, α, Ω, θ_a, S represent the Frank-Kamenetskii parameter, Prandtl number, Biot number, activation energy parameter, material parameter, non-Newtonian parameter, pressure gradient parameter, Darcy number, variable viscosity parameter, viscous heating parameter, ambient temperature parameter and porous medium shape parameter, respectively. The other dimensionless quantities of interest are the skin friction (C_f) and the wall heat transfer rate (Nu) given as

$$C_f = -\frac{\mathrm{d}W}{\mathrm{d}y}(1,t), \quad Nu = -\frac{\mathrm{d}\theta}{\mathrm{d}y}(1,t). \tag{13}$$

In the following section, Eqs. (8)–(13) are solved numerically using a semi-implicit finite difference scheme.

3. Numerical solution

Our numerical algorithm is based on the semi-implicit finite difference scheme [15–19]. Implicit terms are taken at the intermediate time level $(N+\xi)$ where $0 \le \xi \le 1$. The discretization of the governing equations is based on a linear Cartesian mesh and uniform grid on which finite differences are taken. We approximate both the second and first spatial derivatives with second-order central differences. The equations corresponding to the first and last grid points are modified to incorporate the boundary conditions. The semi-implicit scheme for the velocity component reads

$$\frac{\partial}{\partial t}\left(W - \delta\frac{\partial^2 W}{\partial y^2}\right) = G - S^2 e^{-\alpha\theta^{(N)}} W^{(N+\xi)} + e^{-\alpha\theta^{(N)}}\frac{\partial^2}{\partial y^2} W^{(N+\xi)} - \left[\alpha e^{-\alpha\theta}\frac{\partial\theta}{\partial y}\frac{\partial W}{\partial y}\right]^{(N)} + 6\gamma\left(\frac{\partial}{\partial y}W^{(N)}\right)^2\frac{\partial^2}{\partial y^2} W^{(N+\xi)}. \tag{14}$$

In Eq. (14) it is understood that $\partial\#/\partial t := (\#^{(N+1)} - \#^{(N)})/\Delta t$. The equation for $W^{(N+1)}$ then becomes

$$-r_1 W_{j-1}^{(N+1)} + r_2 W_j^{(N+1)} - r_1 W_{j+1}^{(N+1)} = \text{explicit terms}, \tag{15}$$

where

$$r_1 = \frac{1}{\Delta y^2}\left[\delta + \xi\,\Delta t\,(\mu + 6\gamma\dot{\gamma}^2)^{(N)}\right], \quad r_2 = (1 + \xi\,\Delta t\,S^2\,\mu^{(N)} + 2r_1),$$

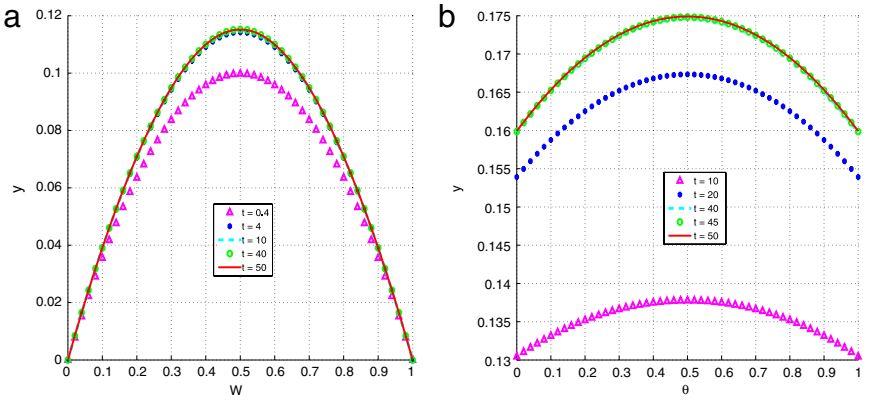

Fig. 2. Transient and steady state profiles.

with $\mu = \exp(-\alpha\theta)$ and $\dot{\gamma} = W_y$. The solution procedure for $W^{(N+1)}$ thus reduces to inversion of tri-diagonal matrices, which is an advantage over a full implicit scheme. The semi-implicit integration scheme for the temperature equation is similar to that for the velocity component. Unmixed second partial derivatives of the temperature are treated implicitly:

$$\Pr \frac{\theta^{(N+1)} - \theta^{(N)}}{\Delta t} = \frac{\partial^2}{\partial y^2}\theta^{(N+\xi)} + \lambda \left\{ \left[(1+\varepsilon\theta)^m \exp\left(\frac{\theta}{1+\varepsilon\theta}\right) \right]^{(N)} + \Omega \left[S^2 W^2 \mathrm{e}^{-\alpha\theta} + \dot{\gamma}^2 \left(\mathrm{e}^{-\alpha\theta} + 2\gamma\dot{\gamma}^2 \right) \right]^{(N)} \right\}. \tag{16}$$

The equation for $\theta^{(N+1)}$ thus becomes

$$-r\,\theta_{j-1}^{(N+1)} + (\Pr + 2r)\,\theta_j^{(N+1)} - r\,\theta_{j+1}^{(N+1)} = \text{explicit terms}, \tag{17}$$

where $r = \xi\,\Delta t/\Delta y^2$. The solution procedure again reduces to inversion of tri-diagonal matrices. The schemes (15) and (17) were checked for consistency. For $\xi = 1$, these are first-order accurate in time but second-order accurate in space. The schemes in [17] have $\xi = 1/2$ which improves the accuracy in time to second order. As [18,19] we, however, use $\xi = 1$ here so that we are free to choose larger time steps and still obtain convergence to the steady solutions.

4. Results and discussion

Unless otherwise stated, we employ the parameter values:

$G = 1$, $\Pr = 10$, $\theta_a = 0.1$, $\delta = 0.1$, $\lambda = 0.1$, $\mathrm{Bi}_1 = 1$, $\mathrm{Bi}_2 = 1$, $m = 0.5$, $\varepsilon = 0.1$, $\alpha = 0.1$, $\Omega = 0.1$, $\gamma = 0.1$, $S = 1$, $\Delta y = 0.02$, $\Delta t = 0.01$ and $t = 40$.

These will be the default values in this work and hence in any graph where any of these parameters is not explicitly mentioned, it will be understood that such parameters take on the default values.

4.1. Transient and steady flow profiles

We display the transient solutions in Fig. 2. The figures show a transient increase in both fluid velocity, Fig. 2(a), and temperature, Fig. 2(b), until a steady state is reached.

4.1.1. Blow-up of solutions

We need to point out early on that depending on certain parameter values in the problem, the steady temperature and velocity profiles, such as those shown in Fig. 2, may not be attainable. In particular, the reaction parameter λ will need to be carefully controlled as "large" values can easily lead to blow-up of solutions as illustrated in Fig. 3.

As shown in Fig. 3, larger values of λ would lead to finite time temperature blow-up since the terms associated with λ are strong heat sources.

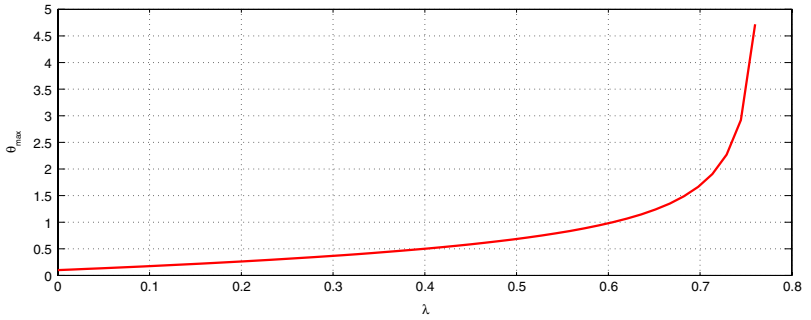

Fig. 3. Blow-up of the fluid temperature for large λ at time $t = 4$.

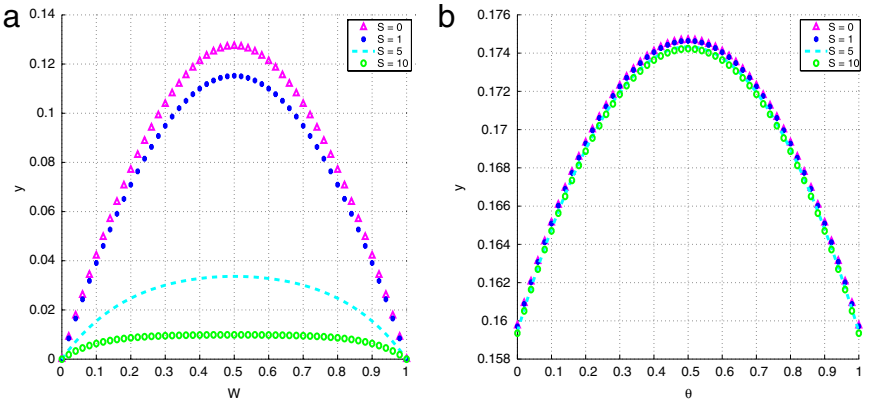

Fig. 4. Effects of the porous medium parameter, S.

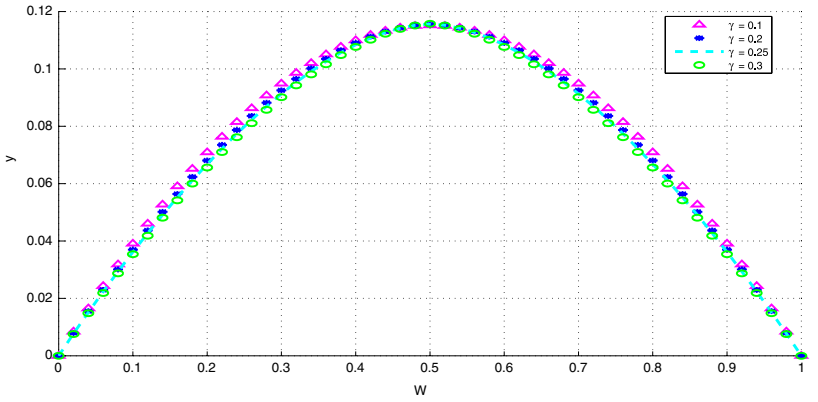

Fig. 5. Effects of the non-Newtonian parameter (γ) on the velocity.

4.1.2. The parameter dependence of solutions

The response of the velocity and temperature to varying values of the porous medium parameter (S) is illustrated in Fig. 4.

An increase in the porous medium parameter S leads to corresponding increases in damping properties in the flow due to reduced porosity. This results in increased resistance to flow and thus explains the reduction in fluid velocity with increasing porous medium parameter as shown in Fig. 4(a). The reduced velocity in turn decreases the viscous heating source terms in the temperature equation and hence correspondingly decreases the fluid temperature as shown in Fig. 4(b).

The response of the velocity to varying values of the non-Newtonian parameter (γ) is illustrated in Fig. 5.

An increase in the parameter γ leads to corresponding increases in those non-Newtonian properties of the fluid, say (visco)elasticity, that would result in increased resistance to flow and thus explain the slight reduction in fluid velocity with increasing non-Newtonian character as measured by the parameter γ; see Fig. 5. The reduced velocity in turn decreases the viscous heating source terms in the temperature equation and hence correspondingly decreases the fluid temperature.

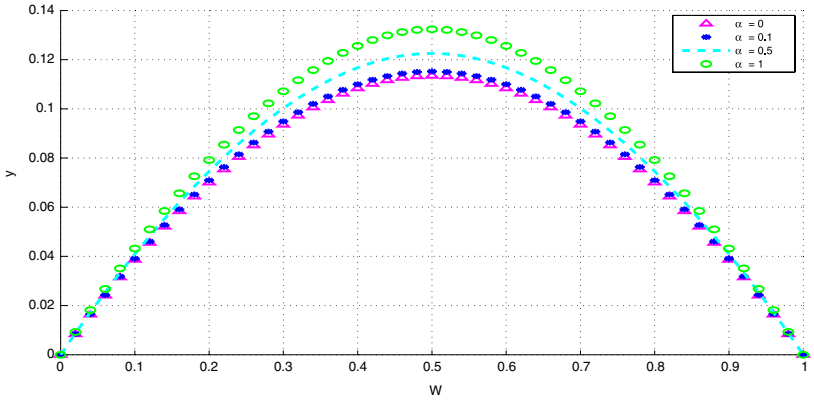

Fig. 6. Effects of the variable viscosity parameter (α) on the velocity.

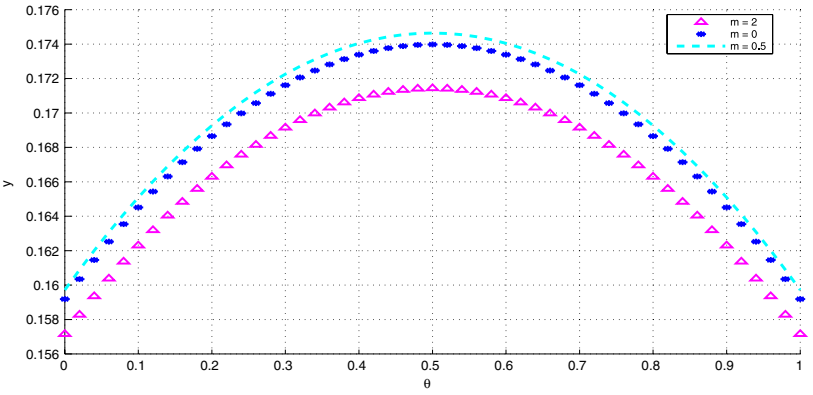

Fig. 7. Effects of the parameter m on the temperature.

Since however the parameter γ only enters the temperature equation implicitly through the velocity field, the effects of γ on the fluid temperature are not as noticeable as those on the fluid velocity.

The influence of the variable viscosity parameter on the velocity profile is shown in Fig. 6. Increasing the parameter α reduces the fluid viscosity and hence correspondingly diminishes the fluid's resistance to flow. This necessarily leads to increased fluid velocity as illustrated in Fig. 6. The increased velocity in turn increases the viscous heating source terms in the temperature equation and hence correspondingly increases the fluid temperature. However, as with the non-Newtonian parameter, the viscous effects are more pronounced in the velocity equation than in the temperature equation and this explains why the effects of α on the fluid temperature are not as noticeable as in the fluid velocity.

The effects of the chemical kinetics exponent m on the temperature profile are shown in Fig. 7.

Fig. 7 shows that the internal heat generated in the fluid during a bimolecular type of exothermic chemical reaction ($m = 0.5$) is higher than that generated under reaction of either the Arrhenius ($m = 0$) or the sensitized ($m = -2$) type. This is so since an increase in the parameter m leads to corresponding increases in the strengths of the chemical reaction source terms in the temperature equation. This leads to increased fluid temperatures as shown in Fig. 7. The increased temperature in turn leads to a reduction in fluid viscosity and hence indirectly to increased fluid velocity. Since however the parameter m only enters the velocity equation implicitly through the temperature/viscosity coupling, the effects of m on the fluid velocity look at best marginal and are not as pronounced as on the fluid temperature.

The effects of the activation energy parameter ε on the temperature profile are shown in Fig. 8. The parameter ϵ plays a more-or-less similar role (both mathematically and physically) to the parameter m described earlier in Fig. 7 and hence its effects are similarly explained.

The graphs of Fig. 8 correspond to the case of bimolecular reactions ($m = 0.5$). It should however be noted that in the cases of sensitized and Arrhenius reactions (in which $m \leq 0$) both temperature and velocity are expected to decrease with increasing ε; see Fig. 9(a) and (b).

This is due to the fact that the function

$$(1 + \varepsilon\theta)^m \exp\left(\frac{\theta}{1 + \varepsilon\theta}\right), \quad m \leq 0,$$

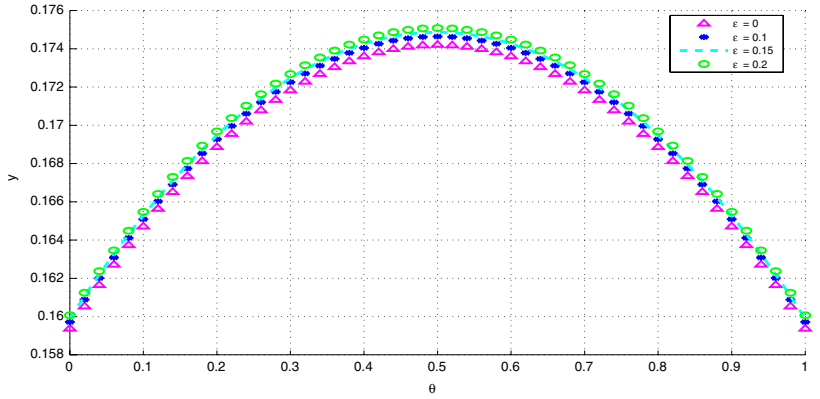

Fig. 8. Effects of the activation energy parameter (ε) on the temperature.

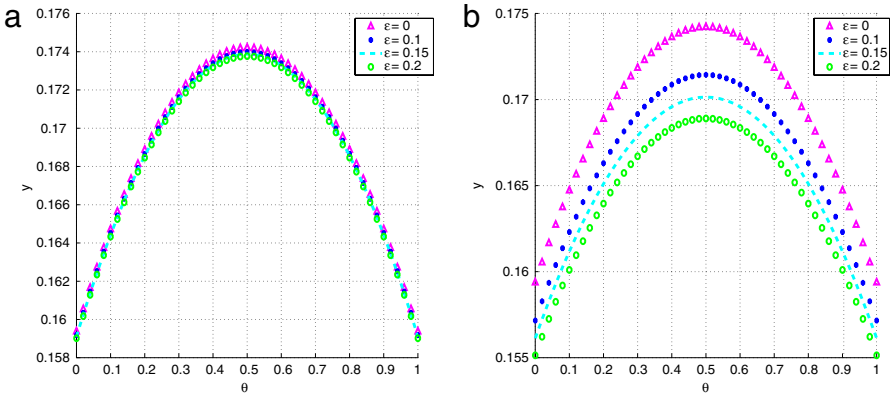

Fig. 9. Effects of the activation energy parameter (ε) on temperature, for $m = 0$ and $m = -2$.

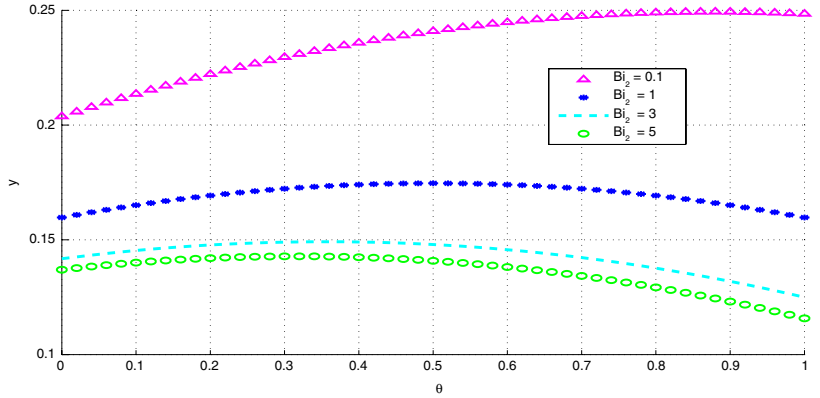

Fig. 10. Effects of the Biot number (Bi_2) on the temperature.

decreases as ε increases. Since this function represents source terms in the temperature equation, the fluid temperature, as expected, decreases with increasing ε, so the maximum temperature is recorded for $\varepsilon = 0$ as shown in Fig. 9(a) and (b).

The effects of the Biot number Bi_2 on the temperature profile are illustrated in Fig. 10.

As seen from the temperature boundary condition (12), higher Biot numbers mean correspondingly higher degrees of convective cooling at the channel walls and hence lead to lower temperatures at the channel walls and hence also in the bulk fluid. The overall temperature profiles thus decrease with increasing Biot number as the bulk fluid continually adjusts to the lower wall temperatures. The reduced temperatures correspondingly decrease the fluid viscosity and hence also marginally decrease the fluid velocity through the viscosity coupling. As noted earlier, such a coupling depending on other parameters

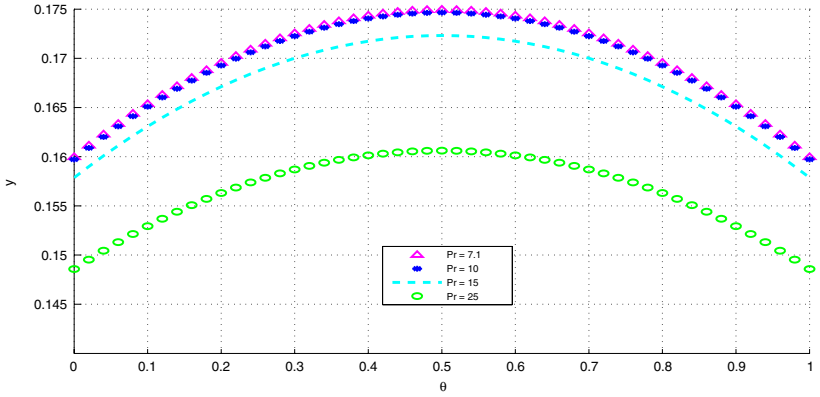

Fig. 11. Effects of the Prandtl number (Pr) on the temperature.

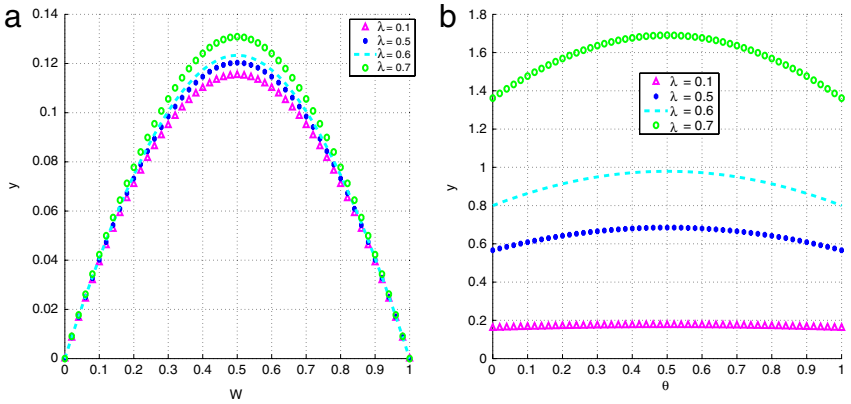

Fig. 12. Effects of the reaction parameter, λ.

as well (say α) does not necessarily result in drastic changes in velocity profiles even though the temperature profiles show well pronounced changes.

The effects of the Prandtl number Pr on the temperature profile are illustrated in Fig. 11.

Larger values of the Prandtl number correspondingly decrease the strength of the source terms in the temperature equation and hence in turn reduce the overall fluid temperature, as clearly illustrated in Fig. 11. As pointed out earlier, the reduced temperature results in decreased fluid viscosity and hence (implicitly) reduces the fluid velocity. The effects of the Prandtl number on the velocity are however, as expected and previously explained, quite marginal.

The effects of the reaction parameter λ on the velocity and temperature profiles are illustrated in Fig. 12.

The reaction parameter λ plays a roughly opposite role to the Prandtl number just described. Increased values of λ lead to significant increases in the reaction and viscous heating source terms and hence significantly increase the fluid temperature as shown in Fig. 12(b) and also in the blow-up Fig. 3. The significant temperature rise in response to the increased λ means that the viscosity coupling to the velocity is no longer weak and hence significant reductions in the viscosity lead to appreciable increases in the fluid velocity, as shown in Fig. 12(a).

The effects of the viscous heating parameter Ω on the temperature profile are illustrated in Fig. 13.

The effects of Ω mirror those of λ, albeit on a smaller scale since Ω is not connected to the exponentially increasing reaction source terms but only to the viscous heating terms.

The wall shear stress dependence on the reaction parameter λ is illustrated in Fig. 14(a) for varying values of the viscosity variation parameter α. Similarly, the wall heat transfer rate dependence on λ is illustrated in Fig. 14(b) for varying values of α.

Fig. 15(a) shows the wall shear stress dependence on λ for varying values of the non-Newtonian parameter γ and similarly, Fig. 15(b) shows the wall shear stress dependence on λ for varying values of the porous medium parameter S. In general, parameters that decrease (increase) the fluid velocity correspondingly decrease (increase) the wall shear stress respectively.

Both the wall heat transfer dependence on λ for varying values of the non-Newtonian parameter γ and the wall heat transfer dependence on λ for varying values of the porous medium parameter S are similar to the behavior illustrated in Fig. 14(b). As with the wall shear stress, parameters that decrease (increase) the fluid temperature correspondingly decrease

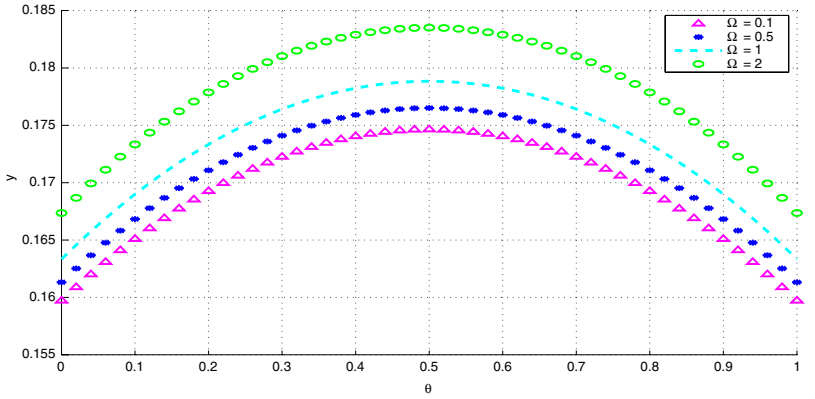

Fig. 13. Effects of the viscous heating parameter (Ω) on the temperature.

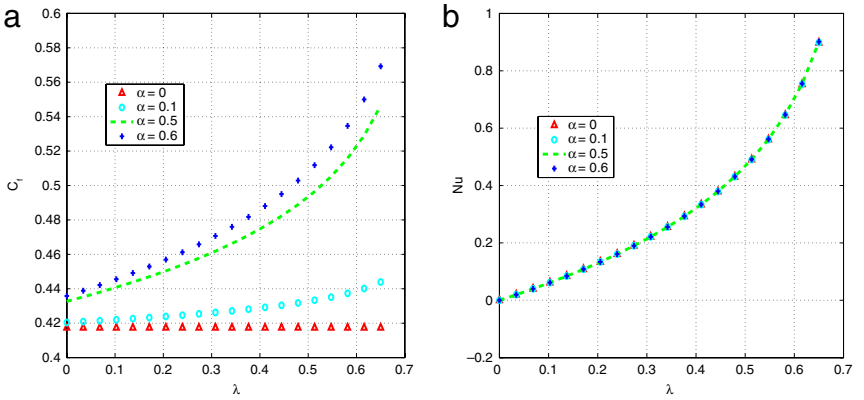

Fig. 14. Variation, with λ and α, of (a) the wall shear stress and (b) the wall heat transfer rate.

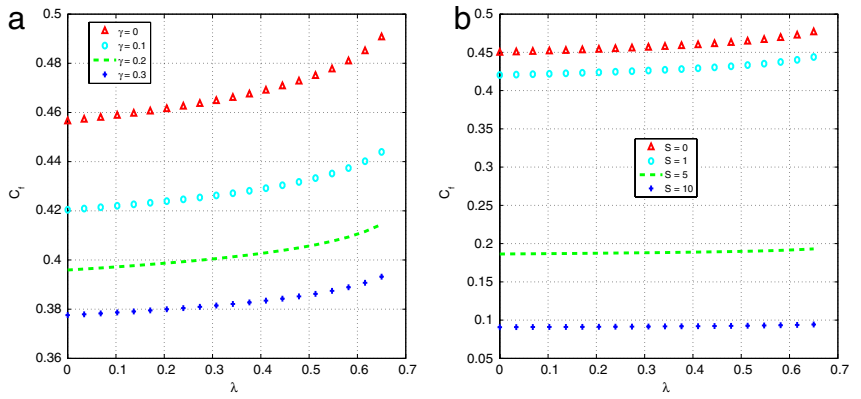

Fig. 15. Variation of the wall shear stress with (a) λ and γ and (b) λ and S.

(increase) the wall heat transfer. In fact, since both the parameters α and γ only marginally increase the temperature, their effects on the wall heat transfer are also similarly marginal. All the results for the wall shear stress and the wall heat transfer were obtained at time $t = 5$.

5. Conclusion

We computationally investigate the transient flow of a reactive variable viscosity non-Newtonian fluid through a porous saturated medium with asymmetric convective cooling. We observe that there is a transient increase in both fluid velocity and temperature with an increase in the reaction strength, viscous heating and fluid viscosity parameter (which decreases the viscosity). A transient decrease in both fluid velocity and temperature is observed with increase in the non-Newtonian

character and porous medium parameter (which decreases the porosity in the flow). The possible finite time blow-up of solutions means that the reaction strength needs to be carefully controlled. We also notice that due to the nature of the coupling of the source terms, the fluid velocity and temperature either both increase or both decrease, together. Parameters that increase any such source terms would increase these quantities and similarly those that decrease the source terms would correspondingly decrease the flow quantities.

References

[1] H.C. Brinkman, On the permeability of media consisting of closely packed porous particles, Applied Scientific Research A1 (1947) 81–86.
[2] C. Truesdell, W. Noll, The non-linear field theories of mechanics, in: S Flügge (Ed.), Handbuch der Physik, vol. 111, Springer, Berlin, 1965, 3.
[3] K.R. Rajagopal, On Boundary Conditions for Fluids of the Differential Type: Navier–Stokes Equations and Related Non-linear Problems, Plenum Press, New York, 1995, p. 273.
[4] R.L. Fosdick, K.R. Rajagopal, Thermodynamics and stability of fluids of third grade, Proceedings of The Royal Society of London A339 (1980) 351.
[5] S.K. Som, S.S. Mondal, S.K. Dash, Energy and exergy balance in the process of pulverized coal combustion in a tubular combustor, Journal of Heat Transfer 127 (2005) 1322–1333.
[6] D.A. Frank-Kamenetskii, Diffusion and Heat Transfer in Chemical Kinetics, Plenum Press, New York, 1969.
[7] A.K. Al-Hadhrami, L. Elliott, D.B. Ingham, A new model for viscous dissipation in porous media across a range of permeability values, Transport in Porous Media 53 (2003) 117–122.
[8] A. Aziz, A similarity solution for laminar thermal boundary layer over a flat plate with a convective surface boundary condition, Communications in Nonlinear Science and Numerical Simulation 14 (2009) 1064–1068.
[9] O.D. Makinde, A. Aziz, MHD mixed convection from a vertical plate embedded in a porous medium with a convective boundary condition, International Journal of Thermal Sciences 49 (2010) 1813–1820.
[10] O.D. Makinde, Thermal ignition in a reactive viscous flow through a channel filled with a porous medium, Transactions of ASME, Journal of Heat Transfer 128 (2006) 601–604.
[11] O.D. Makinde, Thermal stability of a reactive viscous flow through a porous-saturated channel with convective boundary conditions, Applied Thermal Engineering 29 (2009) 1773–1777.
[12] A.M. Siddiqui, R. Mahmood, Q.K. Ghori, Thin film flow of a third grade fluid on a moving belt by He's homotopy perturbation method, International Journal of Nonlinear Sciences and Numerical Simulation 7 (1) (2006) 1–8.
[13] M. Massoudi, I. Christe, Effects of variable viscosity and viscous dissipation on the flow of a third grade fluid in a pipe, International Journal of Non-Linear Mechanics 30 (1995) 687.
[14] M. Yurusoy, M. Pakdemirli, Approximate analytical solutions for the flow of a third grade fluid in a pipe, International Journal of Non-Linear Mechanics 37 (2002) 187.
[15] O.D. Makinde, T. Chinyoka, Numerical investigation of transient heat transfer to hydromagnetic channel flow with radiative heat and convective cooling, Communications in Nonlinear Science and Numerical Simulation 15 (12) (2010) 3919–3930.
[16] O.D. Makinde, T. Chinyoka, Transient analysis of pollutant dispersion in a cylindrical pipe with a nonlinear waste discharge concentration, Computers and Mathematics with Applications 60 (3) (2010) 642–652.
[17] T. Chinyoka, Computational dynamics of a thermally decomposable viscoelastic lubricant under shear, Transactions of ASME, Journal of Fluids Engineering 130 (12) (2008) 121201 (7 pages).
[18] T. Chinyoka, Poiseuille flow of reactive Phan–Thien–Tanner liquids in 1D channel flow, Transactions of ASME, Journal of Heat Transfer 132 (11) (2010) 111701 (7 pages).
[19] T. Chinyoka, Suction–injection control of shear banding in non-isothermal and exothermic channel flow of Johnson–Segalman liquids, Transactions of ASME, Journal of Fluids Engineering 133 (7) (2011) 071205 (12 pages).